European Journal of Medicinal Chemistry 225 (2021) 113807

Contents lists available at ScienceDirect

European Journal of Medicinal Chemistry

journal homepage: http://www.elsevier.com/locate/ejmech

Discovery of the first-in-class dual PPARδ/γ partial agonist for the treatment of metabolic syndrome

Zheng Li [a, b, *], Qiang Ren [a, b, c], Zongtao Zhou [a], Zongyu Cai [a], Bin Wang [a], Jing Han [d], Luyong Zhang [a, b, c, e, **]

[a] School of Pharmacy, Guangdong Pharmaceutical University, Guangzhou, 510006, PR China
[b] Key Laboratory of New Drug Discovery and Evaluation of Ordinary Universities of Guangdong Province, Guangdong Pharmaceutical University, Guangzhou, 510006, PR China
[c] Guangzhou Key Laboratory of Construction and Application of New Drug Screening Model Systems, Guangdong Pharmaceutical University, Guangzhou, 510006, PR China
[d] School of Chemistry and Chemical Engineering, Jiangsu Key Laboratory of Green Synthetic Chemistry for Functional Materials, Jiangsu Normal University, Xuzhou, 221116, PR China
[e] Jiangsu Key Laboratory of Drug Screening, China Pharmaceutical University, Nanjing, 210009, PR China

ARTICLE INFO

Article history:
Received 9 July 2021
Received in revised form
24 August 2021
Accepted 24 August 2021

Keywords:
Diabetes
PPAR
Metabolic syndrome
Insulin resistance
Fatty liver

ABSTRACT

The peroxisome proliferator-activated receptors (PPARs) exert vital function in the regulation of energy metabolism, which were considered as promising targets of metabolic syndrome. Until now, PPARδ/γ dual agonist is rarely reported, and thereby the pharmacologic action of PPARδ/γ dual agonist is still unclear. In this study, we identified a dual PPARδ/γ partial agonist **6** (ZLY06) based on the cyclization strategy of PPARα/δ dual agonist GFT505. ZLY06 revealed excellent pharmacokinetic profiles suitable for oral medication. Moreover, ZLY06 markedly improved glucolipid metabolism without weight gain, and alleviated fatty liver by promoting the β-oxidation of fatty acid and inhibiting hepatic lipogenesis. In contrast, weight gain and hepatic steatosis were observed in Rosiglitazone, a widely used PPARγ full agonist. All of these results indicated that ZLY06 exhibits potential benefits on metabolic syndrome, while no adverse effects related to PPARγ full agonist.

© 2021 Elsevier Masson SAS. All rights reserved.

1. Introduction

Metabolic syndrome affects around 25% of adults worldwide, which including obesity, hyperlipemia, diabetes and fatty liver [1,2]. With the change of lifestyle, the prevalence of metabolic syndrome is increasing and becoming major health burden in the world [3]. Therefore, the development of novel drugs of metabolic syndrome with better efficacy and safety are urgently needed [4]. The peroxisome proliferator-activated receptors (PPARs) exert vital function in the regulation of energy metabolism [5–7]. PPARα, PPARβ/δ, and PPARγ are three isoforms of PPARs. The activation of PPARα or PPARδ improves glucose and lipid metabolism by up-regulating genes of fatty acid β-oxidation [8–10]. Moreover, PPARδ restores function of impaired pancreatic β cells [11], and improves energy metabolism by up-regulating GLP-1 receptor [12]. PPARγ could improve insulin resistance and lipid metabolism by up-regulating fatty acid transport [13]. Currently, many synthetic PPARs agonists, especially for dual or pan PPARs agonists, are in clinical studies of metabolic syndrome, such as dyslipidaemia, fatty liver and type 2 diabetes [14–16]. There are many multiple agonists such as PPARα/δ (GFT505), PPARα/γ (Saroglitazar), and PPARα/δ/γ pan agonists (Lanifibranor) have been identified (Fig. 1) [17]. Our previous studies have also identified several PPAR agonists [18–21]. However, PPARδ/γ dual agonist is rarely reported, and thereby the pharmacologic action of PPARδ/γ dual agonist is still unclear.

GFT505 (Elafibranor) is a PPARα/δ dual agonist (Fig. 1) in Phase III of fatty liver, which exerts multiple benefits in serum lipid, insulin resistance, and hepatoprotective effects [22–24]. Using GFT505 as lead compound, conformational restriction was introduced in the α,β-unsaturated ketone scaffold by cyclization (Fig. 2). Moreover, the easily oxidized methylthioyl group was replaced by a more stable alkoxy. Unexpectedly, the first-in-class PPARδ/γ dual

* Corresponding author. School of Pharmacy, Guangdong Pharmaceutical University, Guangzhou, 510006, PR China.
** Corresponding author. School of Pharmacy, Guangdong Pharmaceutical University, Guangzhou, 510006, PR China.
E-mail addresses: li.zheng.sky@163.com (Z. Li), lyzhang@cpu.edu.cn (L. Zhang).

https://doi.org/10.1016/j.ejmech.2021.113807
0223-5234/© 2021 Elsevier Masson SAS. All rights reserved.

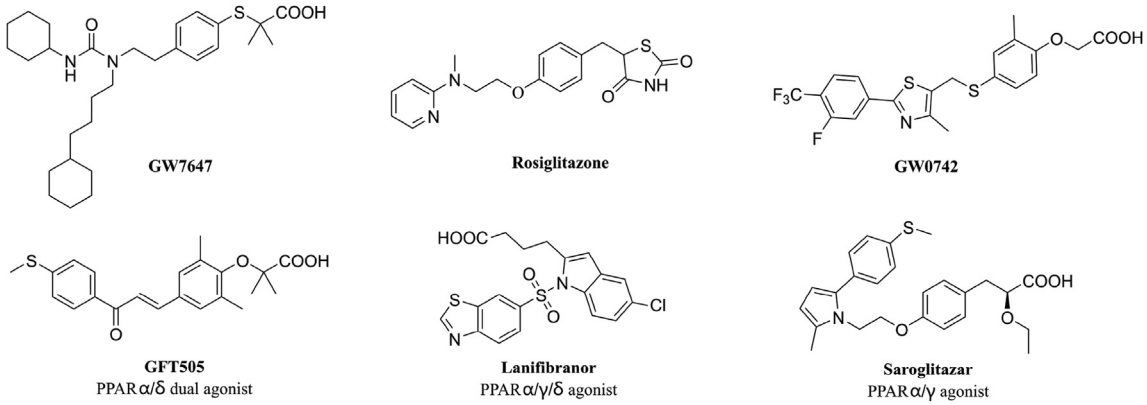

Fig. 1. Structure of representative PPARα, PPARγ and PPARδ agonists.

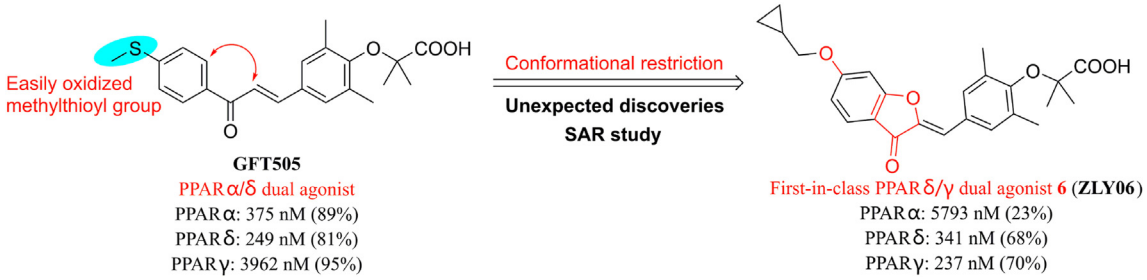

Fig. 2. Our design strategy on structural optimization of GFT505, which resulted in the unexpected discoveries of the first-in-class PPAR δ/γ dual agonist **6** (ZLY06).

partial agonists have been identified based on our design strategy of conformational restriction. Notably, currently available PPARγ full agonists such as Rosiglitazone have side effects including hepatic steatosis, fluid retention, weight gain, and cardiovascular risk. In contrast, PPARγ partial agonists have similar benefits on metabolic syndrome, while no or less incidence of these adverse effects related to PPARγ full agonists [25,26]. Indeed, the optimal PPARδ/γ dual partial agonist **6** (ZLY06) exhibits significant improvement on glucose and lipid metabolism without weight gain and hepatic steatosis observed in Rosiglitazone group. Herein, the structure-activity relationship (SAR) of the present series, molecular modeling, pharmacokinetic profiles and pharmacologic action were described.

2. Results and discussion

2.1. Chemistry

Compounds **1**–**12** were obtained as described in Scheme 1. Alkylation of **1a** with alkyl halide under the standard method of Williamson ether synthesis supplied intermediates **2a**-**g**, which were converted into aurones **4a**-**g** exclusively in Z-configuration under alkali conditions [27]. Alkylation of **4a**-**g** with methyl chloroacetate or methyl 2-bromo-2-methylpropanoate by using potassium carbonate as acid binding agent, followed by hydrolysis under basic condition, received compounds **1**–**12**.

2.2. SAR study

The synthetic compounds were evaluated by using cell-based assays. For PPARα, δ, and γ potencies, the references were GW7647, GW0742, and Rosiglitazone, respectively. As shown in Table 1, replacing chalcone of GFT505 with aurone scaffold led to compound **1**, which revealed reduced potency on PPARα, while improving activity on PPARγ. Interestingly, ethyoxyl analog **2** revealed significantly increased potencies on PPARδ/γ and further decreased activity on PPARα compared to compound **1**, and thereby exhibited a better selectivity against PPARα. Based on this positive result, a series of alkoxy (compounds **3**–**7**) were introduced to explore the tolerability of substituents in this area. Incorporation of

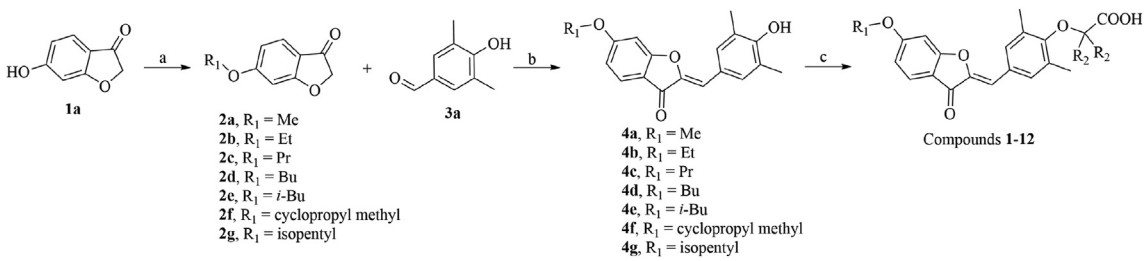

Scheme 1. Reagents and conditions: (a) Alkyl halide, K_2CO_3, acetonitrile, KI, 45 °C, 12 h; (b) DMF, EtOH, KOH, r.t., 38%–48%; (c) Methyl chloroacetate or methyl 2-bromo-2-methylpropanoate, K_2CO_3, acetonitrile, KI, 45 °C, 12 h, and then LiOH·H_2O, THF/MeOH/H_2O, r.t., 4 h, 38%–65%.

Table 1
Activities on PPARα/δ/γ.

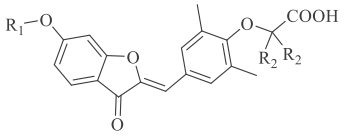

Compd.	R_1	R_2	EC_{50} (nM)		
			*h*PPARα (max%)[a]	*h*PPARγ (max%)	*h*PPARδ (max%)
GW7647			9 (100%)	ND	ND
Rosiglitazone			ND	156 (100%)	ND
GW0742			ND	ND	18 (100%)
GFT505			375 (89%)	3962 (95%)	249 (81%)
1	Me	Me	3680 (18%)	634 (61%)	913 (42%)
2	Et	Me	4635 (14%)	285 (68%)	372 (58%)
3	*n*-Pr	Me	6914 (19%)	412 (64%)	539 (60%)
4	*n*-Bu	Me	5024 (24%)	335 (55%)	413 (60%)
5		Me	5316 (26%)	503 (59%)	652 (65%)
6 (ZLY06)		Me	5793 (23%)	237 (70%)	341 (68%)
7		Me	7725 (12%)	764 (57%)	958 (53%)
8	Me	H	>10,000	1579 (25%)	3217 (18%)
9	Et	H	>10,000	1323 (30%)	2203 (24%)
10	*n*-Pr	H	>10,000	3962 (30%)	3512 (27%)
11		H	>10,000	1745 (29%)	2679 (26%)
12		H	>10,000	1063 (35%)	1523 (32%)

b ND: no data.
[a] EC_{50} value represents the mean of three determinations, max% is the maximal agonist activity of tested compound compared with positive control GW7647, Rosiglitazone, and GW0742, respectively. The max% of positive control GW7647, Rosiglitazone, and GW0742 are set as 100%.

branched alkanes (**5** and **7**) resulted in reduced potency compared to that of straight-chain alkanes (**3** and **4**). Interestingly, the cyclopropyl methyl analog **6** (ZLY06) revealed best balance of activities on PPARδ/γ and best selectivity for PPARα in this series. More importantly, the partial activities of compound **6** (68% for PPARδ, 70% for PPARγ) might reduce side effects induced by full agonist [25]. Further SAR study was also explore the phenoxyacetic acid moiety (compounds **8**–**12**), while their agonistic activities were rather low, indicating the importance of methyl groups in phenoxyacetic acid moiety for the activities of PPAR.

2.3. Docking study

To elucidate the activity and selectivity of compound **6** on different isoforms of PPAR, we carried out a docking study based on X-ray structure of PPARα (3vi8), PPARδ (1GWX) and PPARγ (2Q8S). However, the overly rigid conformation of compound **6** did not match with the "U"-shaped pocket of PPARα, rationally explained that the high selectivity against PPARα. In contrast, dual agonist **6** matched well with binding cavity of PPARδ and PPARγ (Fig. 3). For PPARδ (Fig. 3A), phenoxyacetic acid of **6** generated four hydrogen bonds with amino acid His449, Tyr473 and His323. Besides, cyclopropyl methyl group is inserted into a small hydrophobic cavity, and oxygen atom formed hydrogen bond with Thr288. The binding insight of **6** in PPARδ is very close to that in PPARγ (Fig. 3B), phenoxyacetic acid of compound **6** formed strong interaction with residues His449, Tyr473 and His323. Furthermore, two hydrogen bonds were engendered between oxygen atom of cyclopropyl methoxy and Arg288. Therefore, it can be seen that compound **6** has good activity on both PPARδ and PPARγ, while exhibiting high selectivity against PPARα.

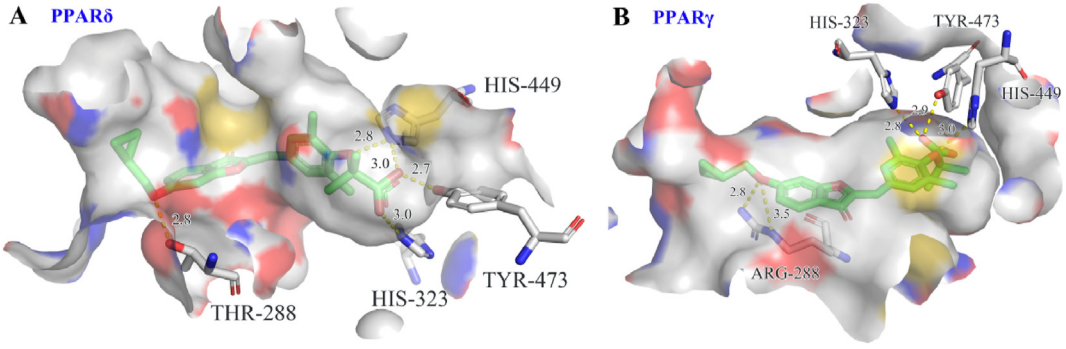

Fig. 3. The binding model of compound **6** in PPARδ (A) and PPARγ (B). Key residues are labeled in black, and hydrogen bonds are represented by yellow dashed lines.

Table 2
Rats PK profile of compound **6**.

Compound	Dose (po)[a]	CL (mL/h/kg)	C_{max} (μg/mL)	AUC_{0-24h} (μg/mL·h)	$T_{1/2}$ (h)
6	3 mg/kg	21.05 ± 6.38	8.67 ± 1.53	51.08 ± 15.26	3.85 ± 1.23

[a] po = oral administration. Results are expressed as mean ± SD for four rats.

2.4. Pharmacokinetic (PK) study

To determine whether oral administration of compound **6** is appropriate, PK parameters are evaluated in SD rats. As shown in Table 2, compound **6** provided considerable PK profile with high plasma exposure. Notably, the C_{max} of compound **6** was 60-fold higher than its EC_{50} values, which ensured sufficient concentration of compound **6** to activate PPARδ and PPARγ *in vivo*. Furthermore, compound **6** has low metabolic clearance and sustained half-life suitable for oral medication.

2.5. Dose-response relationship in HF/STZ mice

The *in vivo* dose-response relationship of compound **6** was evaluated in HF/STZ mice, a diabetic model with insulin deficiency and resistance [28]. In this study, we expect to explore the advantages of partial agonist **6** compared to the full agonist Rosiglitazone. Therefore, Rosiglitazone was selected as positive control, while GFT505 was not selected due to its quite different pharmacological mechanism (PPARα/δ agonist) and structure type compared to PPARδ/γ agonist **6**. After 7-day treatment in HF/STZ model, compound **6** improved glucose tolerance in a dose-response manner. Moreover, the glucose-lowering effects of compound **6** (10 and 20 mg/kg) was equivalent to that of Rosiglitazone, and there was no significant difference between these groups (Fig. 4). These results indicated that the partial agonist may have a similar therapeutic effect with full agonist. Moreover, the dose of 20 mg/kg was identified as a right dosage suitable for exploring long-term studies.

2.6. Chronic effects on ob/ob mice

Based on the dose-response study in HF/STZ mice, we selected the higher dose of compound **6** (20 mg/kg) in further study to explore the safety advantages compared to full agonist Rosiglitazone at a lower dose of 10 mg/kg. A 30-day treatment of compound **6** was performed in *ob/ob* mice, a typical model of metabolic syndrome with obesity, fatty liver and diabetes [29,30]. During treatment, the non-fasting and fasting blood sugar were markedly reduced after 5-day treatment of compound **6** (Fig. 5). Moreover, HbA1c levels, the biomarker of chronic glycemic control, were also markedly reduced in treated groups (Fig. 5F). The diabetic symptoms of polydipsia and polyphagia were dramatically relieved by compound **6**, while food consumption was significantly increased in Rosiglitazone–treated group. After long-term treatment, the adverse effect of gain weight was observed in Rosiglitazone–treated group. Notably, there was no significant difference of body weight between compound **6** and vehicle-treated groups, which might be more beneficial for the treatment of metabolic syndrome compared to Rosiglitazone (Fig. 5E).

After 30-day treatment, compound **6**–treated group significantly reduced the blood lipid level in *ob/ob* mice, including total cholesterol (TC), triglyceride (TG), and low-density lipoprotein (LDL) (Fig. 6). Moreover, the hepatic levels of TG and TC were markedly lower in compound **6**–treated group (Fig. 6E and F). However, Rosiglitazone has no significant effect on plasma LDL, hepatic triglyceride and cholesterol levels (Fig. 6).

Fatty liver is a metabolic syndrome closely related to insulin resistance, obesity, and diabetes. We evaluated whether the fatty liver of *ob/ob* mice could be improved by compound **6**. As shown in Fig. 7C, only a slight improvement of hepatic steatosis in Rosiglitazone-treated group. Notably, compound **6** distinctly alleviated the hepatic steatosis and ballooning (Fig. 7D), suggesting that compound **6** improved fatty liver *in vivo*. In line with the histological change, hepatic function index alanine aminotransferase (ALT) and aspartate transaminase (AST) were markedly lowered in compound **6**-treated group, which was distinctly better than that of Rosiglitazone (Fig. 7E). Indeed, PPARδ agonist could decrease the hepatic function index and steatosis [31]. Quantitative RT-PCR (Fig. 7F) showed that compound **6** significantly up-regulated genes related to PPARδ (*HMGCS2* and *PDK4*), and PPARγ (*GLUT2*, *GK*, and *CD36*). These results suggested that compound **6** exerts therapeutic effects by activating PPARδ and PPARγ *in vivo*. The up-regulation of these lipid metabolism-related genes also indicating that the increased β-oxidation of hepatic fatty acid might

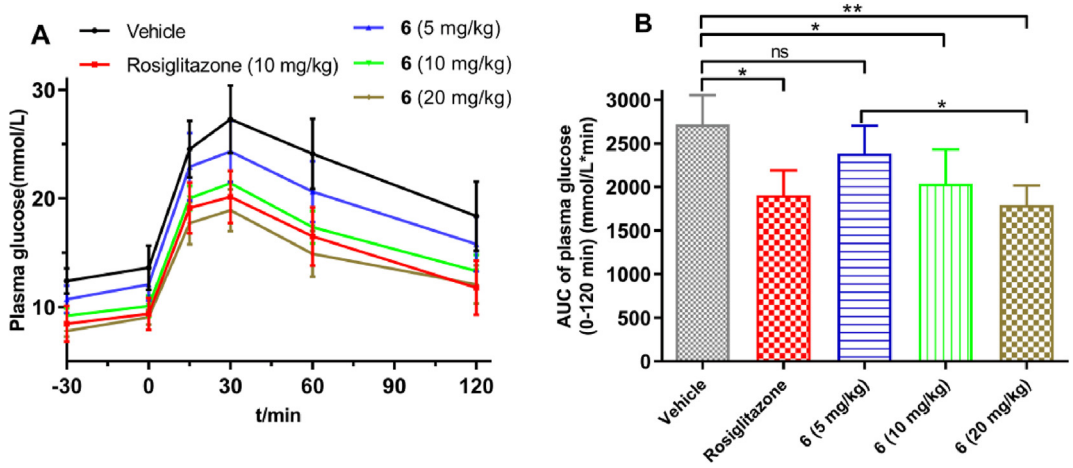

Fig. 4. Dose-response relationship of compound **6** on plasma glucose levels (A) and corresponding $AUC_{0-120min}$ (B) after 7-day treatment in HF/STZ mice. Values are mean ± SD (n = 6). *$p \leq 0.05$ and **$p \leq 0.01$ were analyzed using a one-way ANOVA with Tukey's multiple-comparison post hoc test.

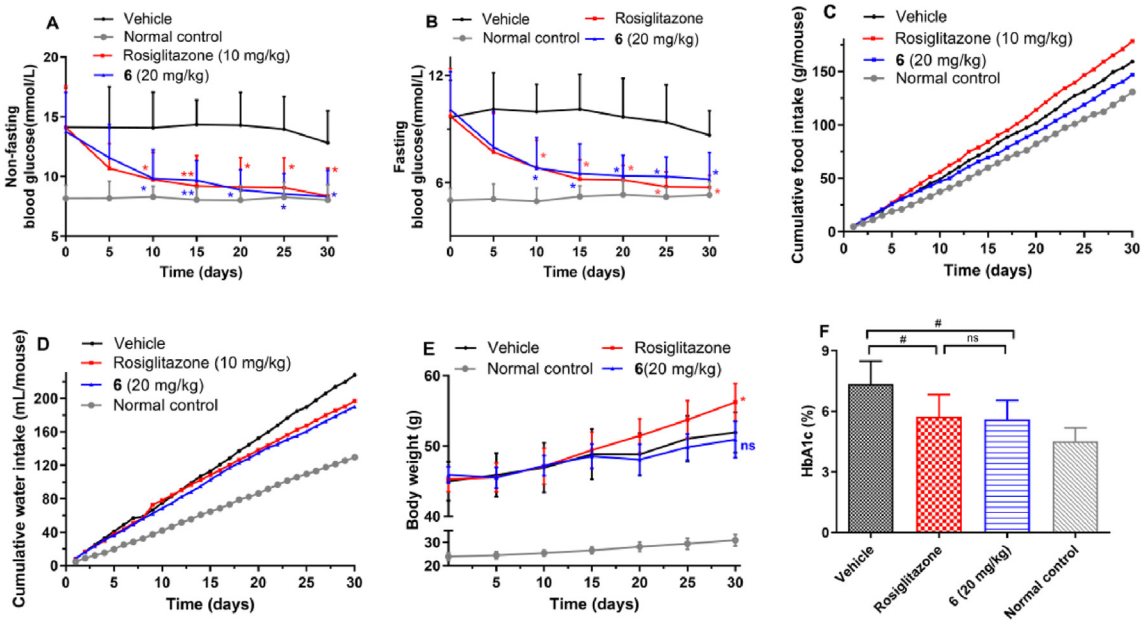

Fig. 5. The plasma glucose levels of non-fasting (A) and fasting (B), cumulative food (C) and water intake (D), body weight (E) and HbA1c (F) in *ob/ob* mice. Values are expressed as mean ± SD (n = 6). $^{*}p \leq 0.05$ and $^{**}p \leq 0.01$ compared to vehicle group by Student's *t*-test. $^{\#}p \leq 0.05$ were analyzed using a one-way ANOVA with Tukey's multiple-comparison post hoc test.

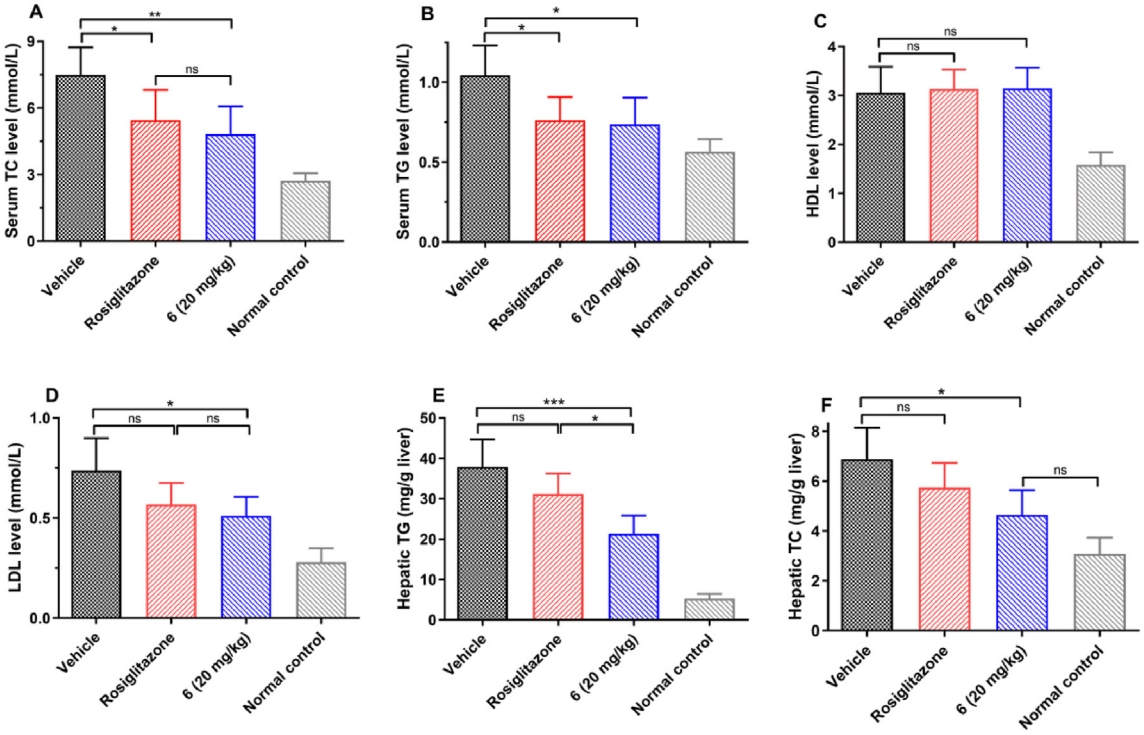

Fig. 6. The plasma levels of TC (A), TG (B), HDL (C) and LDL (D), hepatic levels of TG (E) and TC (F) in *ob/ob* mice. Values are expressed as mean ± SD (n = 6). $^{*}p \leq 0.05$, $^{**}p \leq 0.01$ and $^{***}p \leq 0.001$ were analyzed using a one-way ANOVA with Tukey's multiple-comparison post hoc test.

contributes to the improvement of hepatic steatosis. Moreover, compound **6** significantly decreased the expressions of hepatic lipogenesis-related genes, such as *ADD1*, *ACC*, and *FAS*. On the contrary, Rosiglitazone significantly promoted these genes expressions in liver, partly explaining the reason for weight gain and hepatic steatosis observed in Rosiglitazone group.

3. Conclusion

In conclusion, the first-in-class dual partial agonist **6** (ZLY06) has been discovered based on the strategy of conformational restriction, which has excellent PK profiles. Moreover, compound **6** significantly reduced blood glucose level in HF/STZ and *ob/ob* mice.

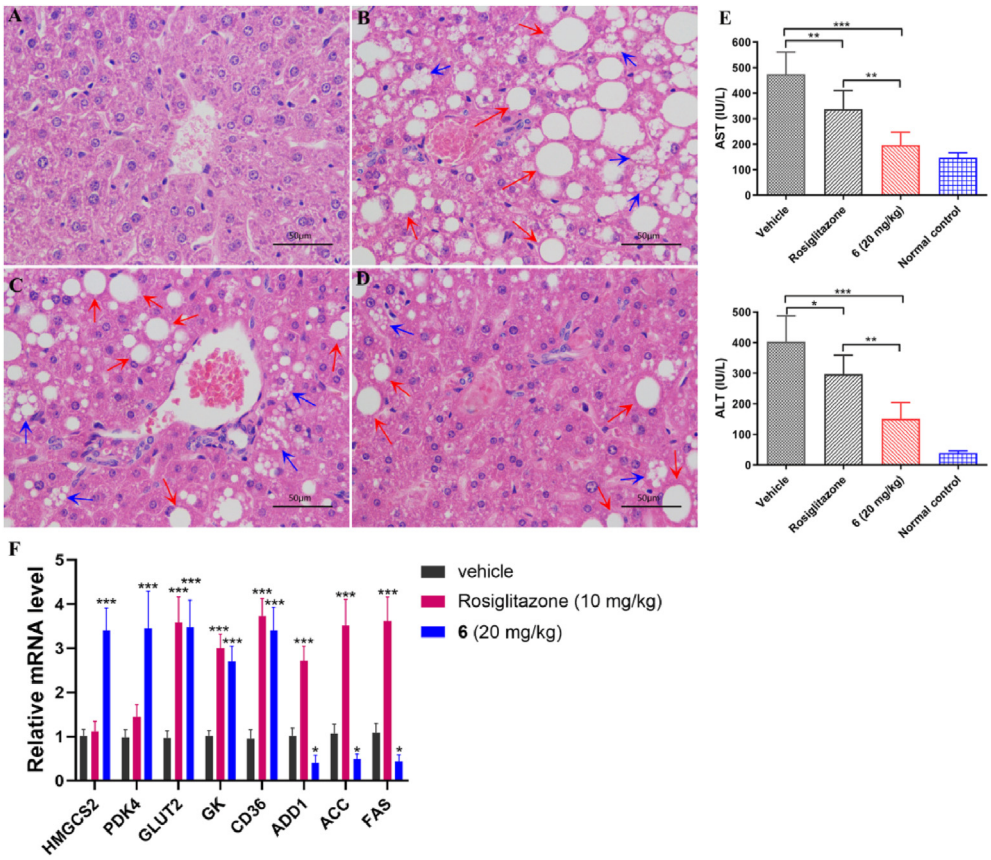

Fig. 7. Representative liver slices (400× magnification) stained with Hematoxylin-Eosin (A: normal control; B: vehicle group; C: Rosiglitazone-treated group; D: compound **6**-treated group). Steatosis: red arrow, ballooning: blue arrow. (E) show the plasma levels of AST and ALT. (F) The relative gene expression levels related to fatty acid oxidation and hepatic lipogenesis. Values are expressed as mean ± SD (n = 6). *$p \leq 0.05$, **$p \leq 0.01$ and ***$p \leq 0.001$ compared to vehicle group were analyzed using a one-way ANOVA with Tukey's multiple-comparison post hoc test.

Notably, dual partial agonist **6** not only exhibited significant improvement on glucolipid metabolism without weight gain, but also alleviated fatty liver by promoting the fatty acid oxidation and inhibiting hepatic lipid accumulation. However, the weight gain and hepatic steatosis were observed in PPARγ full agonist Rosiglitazone. These discoveries indicated dual PPARδ/γ partial agonist **6** (ZLY06) might be a potential candidate of metabolic syndrome.

4. Experimental section

4.1. Chemistry

Reagents and solvents were commercially available without purification. Chromatographic purification was performed on silica gel (200–300 mesh), and monitored by TLC on GF254 plates. Melting points were measured by RY-1 apparatus. ^{1}H and ^{13}C NMR spectra were recorded by Bruker ACF-300Q instrument. High resolution mass spectrometry (HRMS) was performed on AB SCIEX X500R system. Elemental analysis was recorded on Heraeus CHN–O-Rapid analyzer. GW7647, GW0742, GFT505 and Rosiglitazone were purchased from MedChemExpress (Shanghai, China).

4.1.1. General procedure for 4a-g

To a solution of 6-hydroxy-2,3-dihydrobenzo [b]furan-3-one (1 equiv) and halogenated hydrocarbon (1.2 equiv) in acetonitrile was added K_2CO_3 (3 equiv) and catalyzer potassium iodide. After stirred for 12 h at 45 °C, the reaction was filtrated and purified by column chromatography (petroleum ether/ethyl acetate, 20:1) to provide **2a-g**. To the stirred solution of **2a-g** (1 equiv) in 20 mL solvent (ethanol/DMF, 1:1) were added 4-hydroxy-3,5-dimethylbenzaldehyde (1 equiv) and 2.3 mL potassium hydroxide solution (50%). After stirred for 4–6 h, 50 mL water was added to this reaction and adjusting pH to 1–2 using concentrated hydrochloric acid. The reaction was extracted with ethyl acetate and purified by column chromatography (petroleum ether/ethyl acetate, 10:1) to provide **4a-g** as yellow solid.

4.1.1.1. (Z)-2-(4-hydroxy-3,5-dimethylbenzylidene)-6-methoxybenzofuran-3(2H)-one (4a). Yield: 48%; ^{1}H NMR (300 MHz, DMSO-d_6) δ: 8.07 (s, 1H), 7.73–7.61 (m, 3H), 7.15 (d, J = 1.8 Hz, 1H), 6.85, 6.82 (dd, J = 8.7, 2.1 Hz, 1H), 6.68 (s, 1H), 3.95 (s, 3H), 2.32 (s, 6H).

4.1.1.2. (Z)-6-ethoxy-2-(4-hydroxy-3,5-dimethylbenzylidene)benzofuran-3(2H)-one (4b). Yield: 43%; ^{1}H NMR (300 MHz, DMSO-d_6) δ: 8.09 (s, 1H), 7.75–7.62 (m, 3H), 7.09 (s, 1H), 6.83 (d, J = 8.6 Hz, 1H), 6.69 (s, 1H), 4.23 (q, J = 6.8 Hz, 2H), 2.32 (s, 6H), 1.38 (t, J = 6.8 Hz, 3H).

4.1.1.3. (Z)-2-(4-hydroxy-3,5-dimethylbenzylidene)-6-propoxybenzofuran-3(2H)-one (4c). Yield: 38%; ^{1}H NMR (300 MHz, DMSO-d_6) δ: 8.07 (s, 1H), 7.76–7.63 (m, 3H), 7.11 (d, J = 1.6 Hz, 1H), 6.84, 6.81 (dd, J = 8.5, 1.8 Hz, 1H), 6.69 (s, 1H), 4.12 (t, J = 6.5 Hz, 2H), 2.31 (s, 6H), 1.85–1.73 (m, 2H), 1.01 (t, J = 7.4 Hz, 3H).

4.1.2. General procedure for 1-12

To a mixture of **4a-g** (1 equiv) and methyl chloroacetate or methyl 2-bromo-2-methylpropanoate (1.2 equiv) in MeCN was added K_2CO_3 (3 equiv) and catalyzer potassium iodide. After stirred for 12 h at 45 °C, the reaction was filtrated and purified by column chromatography (petroleum ether/ethyl acetate, 10:1) to afford a yellow solid, which was dissolved in 20 mL THF/MeOH/H_2O (2:3:1). Then LiOH·H_2O (4 equiv) was added to above reaction mixture. After stirred for 4 h, the solvent was removed and acidified with diluted hydrochloric acid. After filtered, the residue was purified by column chromatography (petroleum ether/ethyl acetate, 2:1–1:1) to provide **1**–**12** as yellow solid.

4.1.2.1. (Z)-2-(4-((6-methoxy-3-oxobenzofuran-2(3H)-ylidene) methyl)-2,6-dimethylphenoxy)-2-methylpropanoic acid (1). Yield: 52%; m.p. 150–152 °C; ^{1}H NMR (300 MHz, DMSO-d_6) δ: 12.79 (brs, 1H), 7.77–7.52 (m, 3H), 7.10 (s, 1H), 6.83 (d, J = 7.4 Hz, 1H), 6.67 (s, 1H), 3.93 (s, 3H), 2.25 (s, 6H), 1.42 (s, 6H). ^{13}C NMR (75 MHz, DMSO-d_6) δ: 170.30, 164.68, 154.03, 152.84, 150.78, 140.81, 130.14, 128.73, 128.62, 127.53, 116.74, 116.68, 116.45, 111.24, 104.87, 81.29, 66.51, 25.24, 15.45. HRMS (ESI) *m/z*: calcd. for $C_{18}H_{15}O_4$ [M-C$(CH_3)_2$COOH]$^-$: 295.0976; found 295.0972; error: −1.36 ppm. Anal. calcd. For $C_{22}H_{22}O_6$: C, 69.10; H, 5.80; Found: C, 69.35; H, 5.61.

4.1.2.2. (Z)-2-(4-((6-ethoxy-3-oxobenzofuran-2(3H)-ylidene) methyl)-2,6-dimethylphenoxy)-2-methylpropanoic acid (2). Yield: 46%; m.p. 142–144 °C; ^{1}H NMR (300 MHz, DMSO-d_6) δ: 12.78 (brs, 1H), 7.79–7.42 (m, 3H), 7.08 (s, 1H), 6.81 (d, J = 7.9 Hz, 1H), 6.68 (s, 1H), 4.22 (d, J = 6.3 Hz, 2H), 2.25 (s, 6H), 1.41–1.21 (m, 9H). ^{13}C NMR (75 MHz, DMSO-d_6) δ: 182.02, 175.39, 168.43, 167.01, 154.78, 147.19, 133.74, 132.16, 128.00, 125.81, 114.25, 113.57, 111.19, 97.82, 81.27, 65.04, 25.46, 18.13, 14.81. HRMS (ESI) *m/z*: calcd. for $C_{19}H_{17}O_4$ [M-C$(CH_3)_2$COOH]$^-$: 309.1132; found 309.1132; error: 0 ppm. Anal. calcd. For $C_{23}H_{24}O_6$: C, 69.68; H, 6.10; Found: C, 69.44; H, 6.25.

4.1.2.3. (Z)-2-(2,6-dimethyl-4-((3-oxo-6-propoxybenzofuran-2(3H)-ylidene)methyl)phenoxy)-2-methylpropanoic acid (3). Yield: 57%; m.p. 145–147 °C; ^{1}H NMR (300 MHz, DMSO-d_6) δ: 7.69–7.56 (m, 3H), 7.09 (s, 1H), 6.80 (d, J = 8.5 Hz, 1H), 6.67 (s, 1H), 4.08 (t, J = 6.5 Hz, 2H), 2.24 (s, 6H), 1.81–1.68 (m, 2H), 1.38 (s, 6H), 0.98 (t, J = 7.4 Hz, 3H). ^{13}C NMR (75 MHz, DMSO-d_6) δ: 181.97, 175.70, 168.37, 167.11, 155.05, 147.13, 133.77, 132.11, 127.80, 125.74, 114.25, 113.53, 111.26, 97.79, 81.67, 70.70, 25.67, 22.24, 18.19, 10.69. HRMS (ESI) *m/z*: calcd. for $C_{20}H_{19}O_4$ [M-C$(CH_3)_2$COOH]$^-$: 323.1289; found 323.1285; error: −1.24 ppm. Anal. calcd. For $C_{24}H_{26}O_6$: C, 70.23; H, 6.38; Found: C, 70.45; H, 6.31.

4.1.2.4. (Z)-2-(4-((6-butoxy-3-oxobenzofuran-2(3H)-ylidene) methyl)-2,6-dimethylphenoxy)-2-methylpropanoic acid (4). Yield: 51%; m.p. 118–120 °C; ^{1}H NMR (300 MHz, DMSO-d_6) δ: 7.69–7.57 (m, 3H), 7.11 (s, 1H), 6.80 (d, J = 8.6 Hz, 1H), 6.67 (s, 1H), 4.13 (t, J = 6.4 Hz, 2H), 2.22 (s, 6H), 1.78–1.66 (m, 2H), 1.53–1.41 (m, 2H), 1.38 (s, 6H), 0.93 (t, J = 7.5 Hz, 3H). ^{13}C NMR (75 MHz, DMSO-d_6) δ: 182.02, 175.35, 168.42, 167.18, 154.78, 147.18, 133.74, 132.16, 127.97, 125.79, 114.21, 113.61, 111.20, 97.82, 81.25, 69.03, 30.87, 25.46, 19.09, 18.13, 14.09. HRMS (ESI) *m/z*: calcd. for $C_{21}H_{21}O_4$ [M-C$(CH_3)_2$COOH]$^-$: 337.1445; found 337.1441; error: −1.19 ppm. Anal. calcd. For $C_{25}H_{28}O_6$: C, 70.74; H, 6.65; Found: C, 70.85; H, 6.77.

4.1.2.5. (Z)-2-(4-((6-isobutoxy-3-oxobenzofuran-2(3H)-ylidene) methyl)-2,6-dimethylphenoxy)-2-methylpropanoic acid (5). Yield: 42%; m.p. 121–123 °C; ^{1}H NMR (300 MHz, DMSO-d_6) δ: 7.68–7.55 (m, 3H), 7.10 (s, 1H), 6.81 (d, J = 8.6 Hz, 1H), 6.67 (s, 1H), 3.90 (d, J = 6.3 Hz, 2H), 2.23 (s, 6H), 2.06–1.97 (m, 1H), 1.39 (s, 6H), 0.99 (d, J = 6.6 Hz, 6H). ^{13}C NMR (75 MHz, DMSO-d_6) δ: 182.00, 175.39, 168.40, 167.21, 154.79, 147.19, 133.73, 132.16, 127.98, 125.77, 114.25, 113.57, 111.18, 97.83, 81.26, 75.27, 28.01, 25.47, 19.34, 18.13. HRMS (ESI) *m/z*: calcd. for $C_{21}H_{21}O_4$ [M-C$(CH_3)_2$COOH]$^-$: 337.1445; found 337.1450; error: +1.48 ppm. Anal. calcd. For $C_{25}H_{28}O_6$: C, 70.74; H, 6.65; Found: C, 70.56; H, 6.59.

4.1.2.6. (Z)-2-(4-((6-(cyclopropylmethoxy)-3-oxobenzofuran-2(3H)-ylidene)methyl)-2,6-dimethylphenoxy)-2-methylpropanoic acid (6). Yield: 54%; m.p. 141–143 °C; ^{1}H NMR (300 MHz, DMSO-d_6) δ: 7.70–7.58 (m, 3H), 7.07 (s, 1H), 6.81 (d, J = 8.6 Hz, 1H), 6.67 (s, 1H), 3.98 (d, J = 6.9 Hz, 2H), 2.23 (s, 6H), 1.37 (s, 6H), 1.22–1.15 (m, 1H), 0.64–0.56 (m, 2H), 0.40–0.31 (m, 2H). ^{13}C NMR (75 MHz, DMSO-d_6) δ: 181.99, 175.74, 168.39, 167.08, 147.14, 133.79, 132.12, 127.80, 125.74, 114.18, 113.66, 111.28, 97.78, 81.68, 73.90, 25.67, 18.18, 10.26, 3.65. HRMS (ESI) *m/z*: calcd. for $C_{21}H_{19}O_4$ [M-C$(CH_3)_2$COOH]$^-$: 335.1289; found 335.1292; error: +0.89 ppm. Anal. calcd. For $C_{25}H_{26}O_6$: C, 71.07; H, 6.20; Found: C, 71.15; H, 6.27.

4.1.2.7. (Z)-2-(4-((6-(isopentyloxy)-3-oxobenzofuran-2(3H)-ylidene) methyl)-2,6-dimethylphenoxy)-2-methylpropanoic acid (7). Yield: 38%; m.p. 146–148 °C; ^{1}H NMR (300 MHz, DMSO-d_6) δ: 7.69–7.53 (m, 3H), 7.11 (s, 1H), 6.79 (d, J = 8.6 Hz, 1H), 6.67 (s, 1H), 4.14 (t, J = 6.1 Hz, 2H), 2.25 (s, 6H), 1.67–1.58 (m, 2H), 1.32 (s, 6H), 1.21–1.11 (m, 1H), 0.91 (d, J = 6.6 Hz, 6H). ^{13}C NMR (75 MHz, DMSO-d_6) δ: 181.99, 177.53, 174.91, 168.35, 167.08, 156.35, 146.92, 134.13, 131.93, 127.01, 114.33, 113.56, 111.68, 97.81, 84.40, 67.82, 37.57, 26.79, 25.05, 24.03, 22.83, 18.48. HRMS (ESI) *m/z*: calcd. for $C_{22}H_{23}O_4$ [M-C$(CH_3)_2$COOH]$^-$: 351.1602; found 351.1600; error: −0.57 ppm. Anal. calcd. For $C_{26}H_{30}O_6$: C, 71.21; H, 6.90; Found: C, 71.45; H, 6.79.

4.1.2.8. (Z)-2-(4-((6-methoxy-3-oxobenzofuran-2(3H)-ylidene) methyl)-2,6-dimethylphenoxy)acetic acid (8). Yield: 65%; m.p. 243–245 °C; ^{1}H NMR (300 MHz, DMSO-d_6) δ: 7.75–7.62 (m, 3H), 7.13 (d, J = 1.9 Hz, 1H), 6.86, 6.83 (dd, J = 8.6, 2.0 Hz, 1H), 6.69 (s, 1H), 4.45 (s, 2H), 3.94 (s, 3H), 2.31 (s, 6H). ^{13}C NMR (75 MHz, DMSO-d_6) δ: 182.06, 170.55, 168.43, 167.77, 157.19, 147.14, 132.41, 131.59, 128.20, 125.82, 114.40, 113.27, 111.31, 97.57, 69.25, 56.88, 16.65. HRMS (ESI) *m/z*: calcd. for $C_{20}H_{17}O_6$ [M − H]$^-$: 353.1031; found 353.1035; error: +1.13 ppm. Anal. calcd. For $C_{20}H_{18}O_6$: C, 67.79; H, 5.12; Found: C, 67.54; H, 5.23.

4.1.2.9. (Z)-2-(4-((6-ethoxy-3-oxobenzofuran-2(3H)-ylidene) methyl)-2,6-dimethylphenoxy)acetic acid (9). Yield: 61%; m.p. 248–250 °C; ^{1}H NMR (300 MHz, DMSO-d_6) δ: 7.76–7.62 (m, 3H), 7.08 (s, 1H), 6.81 (d, J = 8.5 Hz, 1H), 6.68 (s, 1H), 4.45 (s, 2H), 4.22 (q, J = 6.8 Hz, 2H), 2.31 (s, 6H), 1.39 (t, J = 6.8 Hz, 3H). ^{13}C NMR (75 MHz, DMSO-d_6) δ: 181.97, 170.40, 168.41, 167.02, 157.19, 147.18, 132.37, 131.50, 128.20, 114.31, 112.32, 109.64, 100.35, 69.37, 65.04, 16.61, 14.78. HRMS (ESI) *m/z*: calcd. for $C_{21}H_{19}O_6$ [M − H]$^-$: 367.1187; found 367.1190; error: +0.82 ppm. Anal. calcd. For $C_{21}H_{20}O_6$: C, 68.47; H, 5.47; Found: C, 68.62; H, 5.31.

4.1.2.10. (Z)-2-(2,6-dimethyl-4-((3-oxo-6-propoxybenzofuran-2(3H)-ylidene)methyl)phenoxy)acetic acid (10). Yield: 52%; m.p. 214–216 °C; ^{1}H NMR (300 MHz, DMSO-d_6) δ: 7.76–7.63 (m, 3H), 7.11 (d, J = 1.6 Hz, 1H), 6.84, 6.81 (dd, J = 8.5, 1.8 Hz, 1H), 6.69 (s, 1H), 4.45 (s, 2H), 4.12 (t, J = 6.5 Hz, 2H), 2.31 (s, 6H), 1.85–1.73 (m, 2H), 1.01 (t, J = 7.4 Hz, 3H). ^{13}C NMR (75 MHz, DMSO-d_6) δ: 181.93, 170.42, 167.20, 162.52, 157.15, 147.20, 132.37, 131.51, 128.21, 114.32, 111.16, 109.64, 97.95, 70.77, 69.39, 22.25, 16.63, 10.65. HRMS (ESI) *m/z*: calcd. for $C_{22}H_{21}O_6$ [M − H]$^-$: 381.1344; found 381.1349; error: +1.31 ppm. Anal. calcd. For $C_{22}H_{22}O_6$: C, 69.10; H, 5.80; Found: C, 69.35; H, 5.71.

4.1.2.11. (Z)-2-(4-((6-isobutoxy-3-oxobenzofuran-2(3H)-ylidene) methyl)-2,6-dimethylphenoxy)acetic acid (11). Yield: 57%; m.p. 163–165 °C; ^{1}H NMR (300 MHz, DMSO-d_6) δ: 7.68–7.54 (m, 3H), 7.11 (d, J = 1.7 Hz, 1H), 6.87–6.76 (m, 1H), 6.68 (s, 1H), 4.45 (s, 2H), 3.94 (d, J = 6.5 Hz, 2H), 2.30 (s, 6H), 2.14–2.03 (m, 1H), 1.01 (d, J = 6.7 Hz, 6H). ^{13}C NMR (75 MHz, DMSO-d_6) δ: 181.98, 170.56, 168.41, 167.21, 157.16, 147.16, 132.40, 131.53, 128.21, 125.75, 114.25, 113.55, 111.19, 97.84, 75.27, 69.26, 28.02, 19.35, 16.64. HRMS (ESI) *m/z*: calcd. for $C_{23}H_{23}O_6$ [M − H]$^-$: 395.1500; found 395.1501; error: +0.25 ppm. Anal. calcd. For $C_{23}H_{24}O_6$: C, 69.68; H, 6.10; Found: C, 69.84; H, 6.31.

4.1.2.12. (Z)-2-(4-((6-(cyclopropylmethoxy)-3-oxobenzofuran-2(3H)-ylidene)methyl)-2,6-dimethylphenoxy)acetic acid (12). Yield: 63%; m.p. 172–174 °C; ^{1}H NMR (300 MHz, DMSO-d_6) δ: 12.85 (s, 1H), 7.66–7.56 (m, 3H), 7.09 (s, 1H), 6.83 (d, J = 8.6 Hz, 1H), 6.69 (s, 1H), 4.45 (s, 2H), 4.02 (d, J = 5.7 Hz, 2H), 2.31 (s, 6H), 0.87–0.81 (m, 1H), 0.65–0.58 (m, 2H), 0.42–0.36 (m, 2H). ^{13}C NMR (75 MHz, DMSO-d_6) δ: 181.98, 170.38, 168.44, 167.17, 157.21, 147.22, 132.38, 131.53, 128.22, 125.75, 114.27, 113.63, 111.18, 97.94, 73.89, 69.40, 16.62, 10.28, 3.59. HRMS (ESI) *m/z*: calcd. for $C_{23}H_{21}O_6$ [M − H]$^-$: 393.1344; found 393.1348; error: +1.02 ppm. Anal. calcd. For $C_{23}H_{22}O_6$: C, 70.04; H, 5.62; Found: C, 70.22; H, 5.43.

4.2. PPARα, PPARγ and PPARδ assay

The cell-based assays of PPARα, PPARγ and PPARδ were performed according to our previous reports [18–21]. After transfection for 24 h, test compounds were added and incubated for 18 h. Then each well was lysed with lysis buffer, and added 30 μL Luciferase Assay Reagent II. The firefly and renilla luciferase signal was measured by Promega's Dual Luciferase Reporter Assay System. The values are normalized by Firefly signal/Renilla signal (F/R). The %Activation value is calculated by the following equation: % Activation = [(X-Min)/(Max-Min)] × 100% (X is the "F/R" value in each concentration point. Min is the mean "F/R" value from no compound control. Max is the mean "F/R" value from reference compound control). EC_{50} value was calculated by GraphPad 5.00 (San Diego, CA, USA).

4.3. Docking study

Molecular modeling study was carried out by AutoDock vina 1.1.2. The crystal structures of PPARα (3vi8), PPARδ (1GWX) and PPARγ (2Q8S) were downloaded from PDB database. Firstly, the protein was added polar hydrogen and gasteiger charge, deleted water, and assigned atoms as AD4 based on AutoDockTools. Docking was operated using full flexibility of ligand, and kept other parameters as default values. Pymol 2.3.1 was performed to analyze the molecular modeling results.

4.4. Animals

Eight-week-old male C57BL/6 mice and SD rats were purchased from Guangdong Medical Laboratory Animal Center (Guangdong, China), and eight-week-old male *ob*/*ob* mice were purchased from Model Animal Research Center of Nanjing university (Jiangsu, China). All animals were fed adaptively for 7 days, and feeding chamber was keep under the conditions of 23 ± 2 °C, relative humidity 5 ± 10%, continuous light/dark cycle for 12h. The testing protocols were approved by the ethical committee at Guangdong Pharmaceutical University and conducted according to the Laboratory Animal Management Regulations in China and adhered to guidelines for Care and Use of Laboratory Animals (NIH Publication NO. 85–23).

4.5. Pharmacokinetic studies

The fasted SD rats were orally administered compound **6** (3 mg/kg), and blood was gathered at 5, 15, 30, 45 min and 1, 2, 4, 6, 8, 12, 18, 24 h. The plasma was separated and acetonitrile containing internal standard was added to precipitate proteins. The supernatant was evaluated by LC-MS/MS (Triple Quad 4500, AB SCIEX) to provide the drug concentration. PK profile was analyzed by DAS 2.1.1.

4.6. Dose-effect study in HF/STZ mice

C57BL/6 mice were fed with high–fat diet (45% calories from fat, Mediscience Ltd., China) for four weeks and then injected intraperitoneally with STZ (80 mg/kg). The mice were fed for another four weeks to generate HF/STZ diabetic mice. The fasted HF/STZ mice were orally administered once daily with vehicle, Rosiglitazone (10 mg/kg), or compound **6** (5, 10, and 20 mg/kg) for 7-day treatment. At the end of treatment, fasting mice were administrated with vehicle, Rosiglitazone, or compound **6**. After 30 min, mice were dosed orally with 2 g/kg glucose. Blood was collected at −30, 0, 15, 30, 60 and 120 min post–dose. The plasma glucose was determined using blood glucose test strips (SanNuo ChangSha, China).

4.7. Chronic administration in ob/ob mice

Ob/*ob* mice were orally administered once daily with vehicle, Rosiglitazone (10 mg/kg), or compound **6** (20 mg/kg) for 30 days. Water and diet consumption were measured daily. Body weight, non-fasting and fasting plasma glucose were measured every 5 days. At the end of treatment, alanine aminotransferase (ALT), aspartate transaminase (AST), total cholesterol (TC), triglyceride (TG), high-density lipoprotein (HDL), low-density lipoprotein (LDL) and HbA1c levels were measured using automatic biochemical analyzer (Beckman Coulter, AU5811, Tokyo). Hepatic TG and TC were measured according to the corresponding kits (Nanjing Jiancheng Bioengineering Institute). The liver sections were stained with Hematoxylin-Eosin.

4.8. RT-PCR

RNA was extracted from liver by Trizol Reagent (Invitrogen), and cDNA was synthesized using ReverTra Ace reverse transcriptase (TOYOBO, Japan) on the basic of the operating regulations. RT-PCR was performed with the SYBR Green Realtime PCR Master Mix (TOYOBO, Japan) on iCycler (Bio-rad) accordance with the operating regulations. The gene expressions were calculated by ΔΔCT method and normalized against GADPH mRNA. Primer sequences were as follows: 3-hydroxy-3-methylglutaryl-Coenzyme A synthase 2 (*HMGCS2*) forward primer: AGAGAGCGATGCAGGAAACTT, *HMGCS2* reverse primer: AAGGATGCCCACATCTTTTGG; Pyruvate dehydrogenase kinase 4 (*PDK4*) forward primer: CCGCTTAGTGAACACTCCTTC, *PDK4* reverse primer: TGACCAGCGTGTCTACAAACT; Glucose transporter 2 (*GLUT2*) forward primer: TTCCAGTTCGGCTATGACATCG, *GLUT2* reverse primer: CTGGTGTGACTGTAAGTGGGG; Glycerol kinase (*GK*) forward primer: TGAACCTGAGGATTTGTCAGC, *GK* reverse primer: CCATGTGGAGTAACGGATTTCG; *CD36* forward primer: ATGGGCTGTGATCGGAACTG, *CD36* reverse primer: GTCTTCCCAATAAGCATGTCTCC; Adipocyte determination and diferentiation-dependent factor 1 (*ADD1*) forward primer: GGAACATGGCACCAGACCTTC, *ADD1* reverse primer: AAGGCAGGACTCTGTAGAATCA; Acetyl-CoA carboxylase (*ACC*) forward primer: ACCCACTCCACTGTTTGTGA, *ACC* reverse primer: CCTTGGAATTCAGGAGAGGA; Fatty acid

synthase (*FAS*) forward primer: TAAAGCATGACCTCGTGATGAA, *FAS* reverse primer: GAAGTTCAGTGAGGCGTAGTAG.

4.9. Statistical analysis

GraphPad 5 Software was used to analyze data. General effects analysis used a one-way ANOVA with Tukey's multiple-comparison post hoc test.

Declaration of competing interest

The authors declare no competing financial interest.

Acknowledgments

This study was supported by the Key Field R&D Plan Project of Guangdong province (No. 2019B020201002), Guangdong Basic and Applied Basic Research Foundation (Grant 2019A1515011036), the Natural Science Foundation of Xuzhou (No. KC19154), the Innovative strong school project of Guangdong Pharmaceutical University (Grant 2018KTSCX111), the Innovation Team Projects in Universities of Guangdong Province (No. 2018KCXTD016).

Appendix A. Supplementary data

Supplementary data to this article can be found online at https://doi.org/10.1016/j.ejmech.2021.113807.

References

[1] J. Kaur, A comprehensive review on metabolic syndrome, Cardiol. Res. Pract. 2014 (2014), 943162.
[2] S. O'Neill, L. O'Driscoll, Metabolic syndrome: a closer look at the growing epidemic and its associated pathologies, Obes. Rev. 16 (2015) 1–12.
[3] C.A. Aguilar-Salinas, T. Viveros-Ruiz, Recent Advances in Managing/understanding the Metabolic Syndrome, F1000Research, 2019, p. 8.
[4] C. Villarroel-Vicente, S. Gutiérrez-Palomo, J. Ferri, D. Cortes, N. Cabedo, Natural products and analogs as preventive agents for metabolic syndrome via peroxisome proliferator-activated receptors: an overview, Eur. J. Med. Chem. 221 (2021), 113535.
[5] Z.-H. Zhao, Y.-C. Fan, Q. Zhao, C.-Y. Dou, X.-F. Ji, J. Zhao, S. Gao, X.-Y. Li, K. Wang, Promoter methylation status and expression of PPAR-gamma gene are associated with prognosis of acute-on-chronic hepatitis B liver failure, Clin. Epigenet. 7 (2015).
[6] F. Hong, S. Pan, Y. Guo, P. Xu, Y. Zhai, PPARs as nuclear receptors for nutrient and energy metabolism, Molecules (2019) 24.
[7] B. Gross, M. Pawlak, P. Lefebvre, B. Staels, PPARs in obesity-induced T2DM, dyslipidaemia and NAFLD, Nat. Rev. Endocrinol. 13 (2017) 36–49.
[8] Y.X. Wang, C.H. Lee, S. Tiep, R.T. Yu, J.Y. Ham, H.J. Kang, R.M. Evans, Peroxisome-proliferator-activated receptor delta activates fat metabolism to prevent obesity, Cell 113 (2003) 159–170.
[9] H. Kim, M. Haluzik, Z. Asghar, D. Yau, J.W. Joseph, A.M. Fernandez, M.L. Reitman, S. Yakar, B. Stannard, L. Heron-Milhavet, M.B. Wheeler, D. LeRoith, Peroxisome proliferator-activated receptor-alpha agonist treatment in a transgenic model of type 2 diabetes reverses the lipotoxic state and improves glucose homeostasis, Diabetes 52 (2003) 1770–1778.
[10] X. Palomer, E. Barroso, J. Pizarro-Delgado, L. Pena, G. Botteri, M. Zarei, D. Aguilar, M. Montori-Grau, M. Vazquez-Carrera, PPAR beta/delta: a Key therapeutic target in metabolic disorders, Int. J. Mol. Sci. 19 (2018).
[11] M. Daoudi, N. Hennuyer, M.G. Borland, V. Touche, C. Duhem, B. Gross, R. Caiazzo, J. Kerr-Conte, F. Pattou, J.M. Peters, B. Staels, S. Lestavel, PPAR beta/delta activation induces enteroendocrine L cell GLP-1 production, Gastroenterology 140 (2011) 1564–1574.
[12] Y. Yang, Y. Tong, M. Gong, Y. Lu, C. Wang, M. Zhou, Q. Yang, T. Mao, N. Tong, Activation of PPAR beta/delta protects pancreatic beta cells from palmitate-induced apoptosis by upregulating the expression of GLP-1 receptor, Cell. Signal. 26 (2014) 268–278.
[13] M. Ahmadian, J.M. Suh, N. Hah, C. Liddle, A.R. Atkins, M. Downes, R.M. Evans, PPAR gamma signaling and metabolism: the good, the bad and the future, Nat. Med. 19 (2013) 557–566.
[14] G. Derosa, A. Sahebkar, P. Maffioli, The role of various peroxisome proliferator-activated receptors and their ligands in clinical practice, J. Cell. Physiol. 233 (2018) 153–161.
[15] A.Z. Mirza, Althagafi II, H. Shamshad, Role of PPAR receptor in different diseases and their ligands: physiological importance and clinical implications, Eur. J. Med. Chem. 166 (2019) 502–513.
[16] F. Hong, P. Xu, Y. Zhai, The opportunities and challenges of peroxisome proliferator-activated receptors ligands in clinical drug discovery and development, Int. J. Mol. Sci. 19 (2018).
[17] I. Takada, M. Makishima, Peroxisome proliferator-activated receptor agonists and antagonists: a patent review (2014-present), Expert Opin. Ther. Pat. 30 (2020) 1–13.
[18] Z. Zhou, L. Deng, L. Hu, Q. Ren, Z. Cai, B. Wang, Z. Li, L. Zhang, Hepatoprotective effects of ZLY16, a dual peroxisome proliferator-activated receptor α/δ agonist, in rodent model of nonalcoholic steatohepatitis, Eur. J. Pharmacol. 882 (2020), 173300.
[19] Z. Li, Y. Chen, Z. Zhou, L. Deng, Y. Xu, L. Hu, B. Liu, L. Zhang, Discovery of first-in-class thiazole-based dual FFA1/PPARδ agonists as potential anti-diabetic agents, Eur. J. Med. Chem. 164 (2019) 352–365.
[20] Z. Li, Z. Zhou, F. Deng, Y. Li, D. Zhang, L. Zhang, Design, synthesis, and biological evaluation of novel pan agonists of FFA1, PPARγ and PPARδ, Eur. J. Med. Chem. 159 (2018) 267–276.
[21] Y. Chen, Q. Ren, Z. Zhou, L. Deng, L. Hu, L. Zhang, Z. Li, HWL-088, a new potent free fatty acid receptor 1 (FFAR1) agonist, improves glucolipid metabolism and acts additively with metformin in ob/ob diabetic mice, Br. J. Pharmacol. 177 (2020) 2286–2302.
[22] M.J. Westerouen Van Meeteren, J.P.H. Drenth, E. Tjwa, Elafibranor: a potential drug for the treatment of nonalcoholic steatohepatitis (NASH), Expet Opin. Invest. Drugs (2019) 1–7.
[23] V. Ratziu, S.A. Harrison, S. Francque, P. Bedossa, P. Lehert, L. Serfaty, M. Romero-Gomez, J. Boursier, M. Abdelmalek, S. Caldwell, J. Drenth, Q.M. Anstee, D. Hum, R. Hanf, A. Roudot, S. Megnien, B. Staels, A. Sanyal, Elafibranor, an agonist of the peroxisome proliferator-activated receptor-alpha and -delta, induces resolution of nonalcoholic steatohepatitis without fibrosis worsening, Gastroenterology 150 (2016) 1147–1159.
[24] J.D. Roth, S.S. Veidal, L.K.D. Fensholdt, K.T.G. Rigbolt, R. Papazyan, J.C. Nielsen, M. Feigh, N. Vrang, M. Young, J. Jelsing, L. Adorini, H.H. Hansen, Combined obeticholic acid and elafibranor treatment promotes additive liver histological improvements in a diet-induced ob/ob mouse model of biopsy-confirmed NASH, Sci. Rep. 9 (2019) 9046.
[25] S. Chigurupati, S.A. Dhanaraj, P. Balakumar, A step ahead of PPARgamma full agonists to PPARgamma partial agonists: therapeutic perspectives in the management of diabetic insulin resistance, Eur. J. Pharmacol. 755 (2015) 50–57.
[26] A.A. Amato, S. Rajagopalan, J.Z. Lin, B.M. Carvalho, A.C. Figueira, J. Lu, S.D. Ayers, M. Mottin, R.L. Silveira, P.C. Souza, R.H. Mourao, M.J. Saad, M. Togashi, L.A. Simeoni, D.S. Abdalla, M.S. Skaf, I. Polikparpov, M.C. Lima, S.L. Galdino, R.G. Brennan, J.D. Baxter, I.R. Pitta, P. Webb, K.J. Phillips, F.A. Neves, GQ-16, a novel peroxisome proliferator-activated receptor gamma (PPARgamma) ligand, promotes insulin sensitization without weight gain, J. Biol. Chem. 287 (2012) 28169–28179.
[27] B.A. Brady, M.M. Healy, J.A. Kennedy, W.I. O'Sullivan, E.M. Philbin, The Configuration of Aurones Tetrahedron, vol. 29, 1973, pp. 359–362.
[28] J. Luo, J. Quan, J. Tsai, C.K. Hobensack, C. Sullivan, R. Hector, G.M. Reaven, Nongenetic mouse models of non-insulin-dependent diabetes mellitus, Metabolism 47 (1998) 663–668.
[29] A.J.F. King, The use of animal models in diabetes research, Br. J. Pharmacol. 166 (2012) 877–894.
[30] A. King, J. Bowe, Animal models for diabetes: understanding the pathogenesis and finding new treatments, Biochem. Pharmacol. 99 (2016) 1–10.
[31] H.E. Bays, S. Schwartz, T. Littlejohn III, B. Kerzner, R.M. Krauss, D.B. Karpf, Y.-J. Choi, X. Wang, S. Naim, B.K. Roberts, MBX-8025, A novel peroxisome proliferator receptor-delta agonist: lipid and other metabolic effects in dyslipidemic overweight patients treated with and without atorvastatin, J. Clin. Endocrinol. Metab. 96 (2011) 2889–2897.